MOLECULAR AND CELLULAR BIOLOGY, May 2010, p. 2401–2410 Vol. 30, No. 10
0270-7306/10/$12.00 doi:10.1128/MCB.01275-09

Phospholipase Cγ Activation Drives Increased Production of Autotaxin in Endothelial Cells and Lysophosphatidic Acid-Dependent Regression▽

Eunok Im,[1]† Ruta Motiejunaite,[1,4] Jorge Aranda,[1] Eun Young Park,[1] Lorenzo Federico,[2] Tae-im Kim,[3] Timothy Clair,[5] Mary L. Stracke,[5] Susan Smyth,[2] and Andrius Kazlauskas[1]*

Schepens Eye Research Institute, Harvard Medical School, Boston, Massachusetts 02114[1]; Department of Pharmacology, University of Kentucky, Lexington, Kentucky 40536[2]; Corneal Dystrophy Research Institute, Department of Ophthalmology, Yonsei University College of Medicine, Seoul, South Korea[3]; Department of Biochemistry and Biophysics, Vilnius University, Vilnius, Lithuania[4]; and Laboratory of Pathology, National Cancer Institute, Center for Cancer Research, National Institutes of Health, Bethesda Maryland 20892[5]

Received 21 September 2009/Returned for modification 2 November 2009/Accepted 26 February 2010

We previously reported that vascular endothelial growth factor (VEGF)-dependent activation of phospholipase Cγ1 (PLCγ) regulated tube stability by competing with phosphoinositide 3-kinase (PI3K) for their common substrate. Here we describe an additional mechanism by which PLCγ promoted regression of tubes and blood vessels. Namely, it increased the level of autotaxin (ATX), which is a secreted form of lysophospholipase D that produces lysophosphatidic acid (LPA). LPA promoted motility of endothelial cells, leading to disorganization/regression of tubes *in vitro*. Furthermore, mice that under- or overexpressed members of this intrinsic destabilization pathway showed either delayed or accelerated, respectively, regression of blood vessels. We conclude that endothelial cells can be instructed to engage a PLCγ-dependent intrinsic destabilization pathway that results in the production of soluble regression factors such as ATX and LPA. These findings are likely to potentiate ongoing efforts to prevent, manage, and eradicate numerous angiogenesis-based diseases such as proliferative diabetic retinopathy and solid tumors.

The formation of new blood vessels from the existing vasculature (angiogenesis) is an elegant process that is the subject of intense scientific inquiry. Some of the agents that induce angiogenesis have been identified, and this information has led to development of novel therapies for endemic human diseases. For instance, vascular endothelial growth factor A (VEGF-A) promotes angiogenesis, and approaches to block VEGF-A action are the preferred treatment option for patients with the wet form of macular degeneration (2, 9, 11).

Angiogenesis is a program of deliberately orchestrated cellular events (5). The first step is destabilization of a quiescent vessel that is associated with loss of pericytes. Endothelial cells within the vessel relax their intercellular interactions and migrate out into areas where the surrounding extracellular matrix has been degraded by proteases. Proliferation of endothelial cells and recruitment of circulating endothelial precursors generate the new vessel. In the final step, the new vessel undergoes stabilization and thereby concludes the program.

In contrast to the wealth of information on how angiogenesis is initiated, relatively little is known regarding the regression of vessels. There are several well-known mechanisms for blood vessel regression. The first to be discovered was regression resulting from a decline in the level of proangiogenic factors (1, 3, 20). Vessels can also regress without an obvious shortage of proangiogenic factors (14, 15, 33, 38), and this phenomenon heralds the existence of additional mechanisms. For instance, macrophages and pericytes direct regression of hyaloid vessels by secreting Wnts and angiopoietin 2, respectively (21, 22, 25, 35). Elucidating how vessel stability/regression is governed is likely to guide the development of therapies to induce regression of existing pathological vessels that are an Achilles' heel of human diseases (solid tumors and various eye diseases) that afflict a large number of people worldwide.

One of the intracellular signaling cascades that VEGF triggers is initiated by phospholipase Cγ (PLCγ) (27). Blocking VEGF-dependent activation of PLCγ suppresses many of the cellular events intrinsic to angiogenesis (40), and mice expressing a VEGF receptor unable to activate PLCγ fail to properly organize blood vessels and die *in utero* (37). In an *in vitro* vasculogenesis model in which endothelial cells are the only cell type, VEGF-dependent activation of PLCγ resulted in regression of tubes (14). Together these studies demonstrate that PLCγ is a key effector for VEGF-dependent responses. In addition, they suggest that PLCγ-dependent events govern vessel stability/regression.

Autotaxin (ATX) was originally identified as a tumor cell motility factor and has more recently been implicated in angiogenesis. For instance, ATX-transfected Ras-transformed NIH 3T3 cells or purified ATX increased angiogenesis in an *in vivo* Matrigel plug assay (30). Furthermore, VEGF increases expression of ATX (18, 34); ATX was identified as one of the genes that control the angiogenic response to basic fibroblast growth factor (bFGF) (36). Finally, ATX-deficient mice die during embryogenesis and display a vascular defect (41, 48).

ATX, or nucleotide pyrophosphatase/phosphodiesterase 2 (NPP2), is a plasma lysophospholipase D (lysoPLD), which generates lysophosphatidic acid (LPA) from lysophosphatidyl

* Corresponding author. Mailing address: Schepens Eye Research Institute, Harvard Medical School, 20 Staniford St., Boston, MA 02114. Phone: (617) 912-2517. Fax: (617) 912-0111. E-mail: ak@eri.harvard.edu.

† Present address: Division of Digestive Diseases, David Geffen School of Medicine, UCLA, Los Angeles, CA 90095.

▽ Published ahead of print on 15 March 2010.

choline (LPC) (43, 44). LPA signals through G protein-coupled receptors and is degraded through dephosphorylation by lipid phosphate phosphatases (LPPs) (39, 47). While ATX is implicated in angiogenesis, the ATX-regulated steps of the angiogenic program have not been elucidated.

In this report we describe our serendipitous discovery that the stability/regression of tubes and blood vessels is regulated by an intrinsic destabilization/regression pathway that involves PLCγ, ATX, and LPA.

MATERIALS AND METHODS

Antibodies and reagents. Anti-mouse and anti-rabbit antibodies conjugated to horseradish peroxidase were obtained from Amersham Biosciences (Piscataway, NJ). Rabbit polyclonal anti-Erk antibody was obtained from Cell Signaling Technology (Beverly, MA). Anti-Flag antibody was purchase from Sigma. The RasGAP antibody was crude polyclonal rabbit antiserum that was previously described (45). The anti-ATX antibody (84b) was affinity purified and raised against a peptide in the C terminus of ATX. Cyclosporine (CS) and INCA-6 were purchased from Calbiochem (San Diego, CA). FK-506 was purchased from A.G. Scientific (San Diego, CA). The LPP1 cDNA was a gift from Susan Pyne (Strathclyde Institute of Pharmacy and Biomedical Science, Glasgow, United Kingdom). Recombinant VEGF-A was purchased from Upstate Biotechnology Inc. All other chemicals and reagents were obtained from Sigma (St. Louis, MO) unless otherwise indicated.

Cell culture. Retinal endothelial cells (BRECs) were isolated from bovine eyes as described previously (10, 16). BRECs were maintained in EBM (Lonza, Walkersville, MD) supplemented with 10% horse serum (Clonetics), 80 U/ml penicillin-streptomycin C (Irvine Scientific, Santa Ana, CA), and 12 μg/ml bovine brain extract (Clonetics). The cells were plated on plastic coated with 50 μg/ml bovine fibronectin and incubated at 37°C in 5% CO_2. For all experiments, cells were used between passages 7 and 10. Human intestinal microvascular endothelial cells (HIMECs) were isolated as previously described (4). Briefly, HIMECs were obtained from normal areas of the intestines of patients admitted for bowel resection. HIMECs were isolated by enzymatic digestion and subsequently cultured in MCDB131 medium (Sigma) supplemented with 20% fetal bovine serum (BioWhittaker, Walkersville, MD), antibiotics (BioWhittaker), heparin (Sigma), and endothelial cell growth factor (Roche Applied System, Indianapolis, IN). Cultures of HIMECs were maintained at 37°C in 5% CO_2. HIMECs were used between passages 7 and 12. Human umbilical vein endothelial cells (HUVECs) were purchased from Clonetics and maintained in EGM-2 (Clonetics) with low-serum growth factor supplement (Clonetics). For all experiments, HUVECs were used between passages 5 and 7.

bFGF pellet preparation and corneal micropocket assay. bFGF pellets (80 ng/pellet; R&D Systems, Minneapolis, MN) were made of the slow-release polymer Hydron (polyhydroxyethylmethacrylate), which contained a mixture of 45 ng/pellet of sucralfate (Sigma) as previously described by Kenyon et al. (20). Briefly, a suspension of bFGF and sucralfate was made and dried for 8 min. To this suspension, 10 μl of 12% Hydron in ethanol was added. The suspension was then deposited onto a sterilized nylon mesh (LAB Pak; Sefar America, Depew, NY) and embedded between the fibers. The resulting grid of 10- by 10-mm squares was allowed to dry, and 30 to 40 uniformly sized pellets of 0.4 by 0.4 by 0.2 mm were selected for the assay. Corneal micropockets were created with a modified von Graefe knife. Hydron pellets containing 80 ng of human bFGF were implanted into the corneal pockets. Corneal neovascularization was examined daily and photographed with a slit lamp biomicroscope (Nikon FS-2; Nikon, Tokyo, Japan) on days 0, 7, 14, and 21 after pellet implantation. The blood vessels were quantitated using the NIH Image program (NIH, Bethesda, MD). Statistical analysis was performed with the Student *t* test.

Measurement of hyaloid vessel regression. At postnatal day 1 (P1), P5, P10, P15, and P20, both $PLC\gamma^{+/+}$ and $PLC\gamma^{+/-}$ mice were euthanized, and the eyes were removed, fixed in 4% formaldehyde, and embedded in methyl methacrylate. For $ATX^{Tg/+}$ and $ATX^{+/+}$ mice, the eyes at postnatal days 1, 3, 7,10, and 22 were used. Serial sections (3 to 10 μm) of whole eyes were cut sagitally, through the cornea and parallel to the optic nerve. Sections were stained with hematoxylin and eosin. The total number of hyaloid vessels in 10 slides from each eye was counted by a masked observer. The Student *t* test was used for the statistical analysis.

Migration assay using Boyden chambers. Cell migration was evaluated using a quantitative cell migration assay kit (Millipore, Billerica, MA) following the manufacturer's instructions. Briefly, the Boyden chamber assay kit consists of a hollow plastic chamber sealed at one end with a porous membrane. BRECs were seeded in this hollow chamber in the presence of serum-free medium. The hollow chamber resided in another chamber filled with either vehicle, 10% horse serum, 1 μM LPA, or 25 ng/ml VEGF-A. Cells were allowed to migrate overnight through the pores to the other side of the membrane. The inner tube was then removed and carefully washed, and any nonmigratory cells inside the membrane were carefully scraped away. Cells that had migrated to the opposite side of the membrane were stained, extracted and quantified with a spectrophotometer (Spectra Max M5; Molecular Devices, Sunnyvale, CA).

Time-lapse images. HIMECs were subjected to a tube formation assay. After 6 h, the cells were supplemented with medium containing 10 μM LPA. The culture plate was placed in an incubator that was assembled with an Axio Observer D1 inverted microscope (Carl Zeiss). The temperature inside the incubator was maintained at 37°C with 5% CO_2. Images were captured with an AxioCam digital camera (Carl Zeiss) and processed with Adobe Photoshop.

Tube formation assay. The tube formation assay was performed as previously described (14, 16). The average tube length was routinely 15 to 30 mm in either BRECs or HUVECs exposed to VEGF-A or in platelet-derived growth factor receptor (PDGFR)-expressing BRECs responding to endogenous PDGF.

Transfection of siRNA-ATX oligonucleotides. Small interfering RNA (siRNA) oligonucleotides that target ATX and a nontargeting siRNA pool were purchased from Dharmacon (Lafayette, CO) and resuspended according to the manufacturer's instructions. For transfection, 7×10^4 HUVECs were plated onto solidified collagen gel and incubated for 16 to 18 h in culture medium. siRNA-ATX and siRNA control oligonucleotides at 100 nM were mixed with TransPass R2 transfection reagent (New England BioLabs, Beverly, MA) 20 min before transfection. Cells were washed once with Dulbecco modified Eagle medium (DMEM) (GIBCO BRL, Gaithersburg, MD), and then the transfection reagent mixture was added. After 4 h of incubation, the top collagen gel was added. After 1 h, 2 ml of culture medium was added and the cultures were incubated overnight. Cells were then incubated for an additional 24 h in freshly added culture medium.

Stable expression of PDGFR mutants. The Y40/51 and Y40/51/21 constructs were previously constructed and characterized (46). The PDGFR cDNAs were subcloned into the retroviral vector pLXSN. The pLXSN empty vector and PDGFR mutants/pLXSN constructs were transfected into 293GPG cells. The virus-containing supernatant was collected for 5 days, concentrated (25,000 × *g*, 90 min, 4°C), and used as described previously (31). Cells were infected and selected on the basis of proliferation in the presence of G418 (1 mg/ml).

Western blot analysis and immunoprecipitation. For Western blot analysis of anti-Flag-LPP1, 2×10^6 BRECs were plated into a 10-cm tissue culture plate and incubated for at least 18 h in culture medium. Total cell lysates were prepared and Western blot analysis was performed as described previously (16).

To reprobe a blot, the blot was first stripped by incubating for 30 min at 60°C in a buffer containing 6.25 mM Tris-HCl, pH 6.8, 2% SDS, and 100 mM β-mercaptoethanol and then reprobed with the desired primary antibody.

Western blot analysis of cells that had organized into tubes was performed as follows. Cells were recovered following a collagenase treatment (collagenase type I-S from Sigma; 281 units per well for 20 min at 37°C), which dissolved the collagen gel. The cells were rinsed three times with ice-cold phosphate-buffered saline (PBS), and total cell lysates were made and subjected to Western blot analysis as described above.

Mice. $PLC\gamma^{+/-}$ mice were a gift from Demin Wang (Blood Center of Wisconsin, Milwaukee, WI) (23). $PLC\gamma^{+/-}$ mice and their wild-type (WT) littermates were derived from breeding heterozygotes. $ATX^{Tg/+}$ and $ATX^{+/+}$ mice were generated as previously described (32). All animal studies were approved by the Institutional Animal Care and Use Committee of the Schepens Eye Research Institute (Harvard Medical School) and the University of Kentucky.

RESULTS

Developmental and pathological vessel regression is delayed in $PLC\gamma^{+/-}$ mice. We previously established and described an *in vitro* model of vasculogenesis in which primary endothelial cells organized into tubes in a VEGF-dependent manner (16). After a period of apparent stability, the tubes regressed despite the continued presence of serum and VEGF. Consistent with the idea that regression was not the inevitable consequence of starvation-induced apoptosis, the tubes regressed prior to apoptosis (14). Importantly, regression appeared to be a deliberate

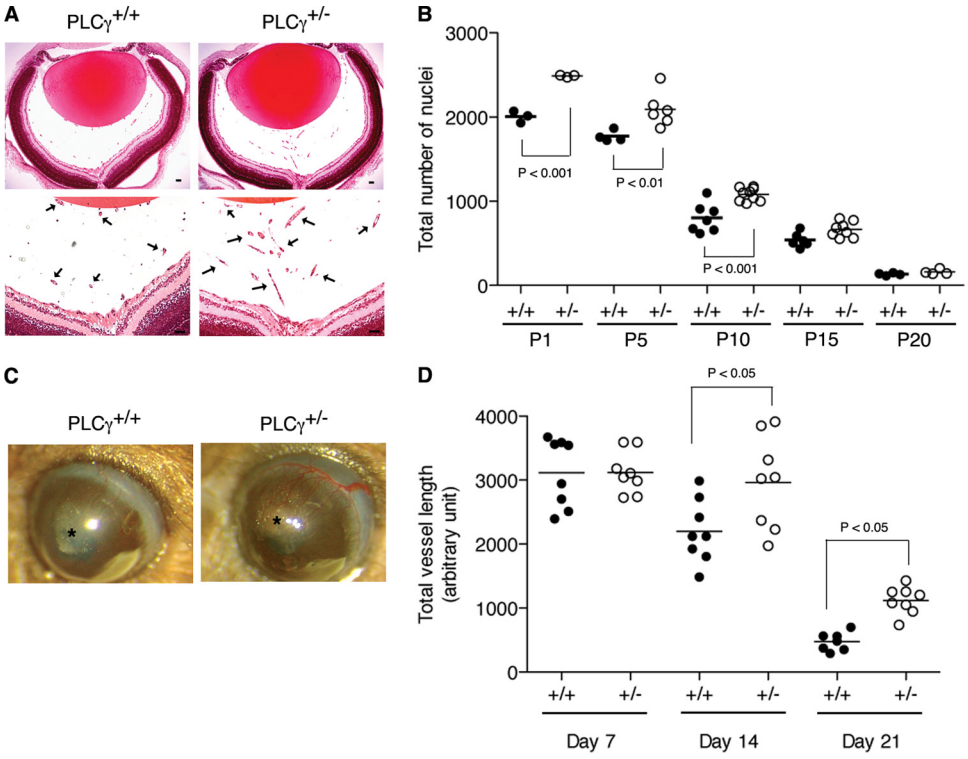

FIG. 1. Regression of hyaloid and corneal vessels is delayed in PLCγ$^{+/-}$ mice. (A) At postnatal days 1, 5, 10, 15, and 20, PLCγ$^{+/-}$ and PLCγ$^{+/+}$ mice were euthanized, and the eyes were removed, fixed, and sectioned. Sections were stained with hematoxylin and eosin; representative sections at postnatal day 5 are shown in the upper panels. High-magnification photos are shown in the lower panels. This section was through the optic nerve and therefore included the major retinal artery. Arrows indicate the hyaloid vessels. The bar is 50 μm. (B) The nuclei of hyaloid vessels in the indicated number of mice were counted; the horizontal bar denotes the average. There were statistically significant differences between the two groups at the first three time points. (C) A bFGF pellet was introduced into the corneas of PLCγ$^{+/-}$ and PLCγ$^{+/+}$ mice, and the neovascular response was photographed at the indicated times. Representative eyes at day 14 are shown. The pellet is to the right of the asterisk. (D) The total vessel length was measured and quantified; each data point represents an individual mouse. Regression was slower in the PLCγ$^{+/-}$ mice, and this difference was statistically significant on days 14 and 21.

response, since it required VEGF-dependent activation of PLCγ (14). To assess whether these *in vitro* principles extended to the *in vivo* setting, we tested whether blood vessel regression was delayed in PLCγ heterozygous mice.

We first compared regression of hyaloid vessels, which is a developmentally driven phenomenon in newborn mice. These vessels are found in the vitreous along the inner limiting membrane of the retina (vasa hyaloidea propria) and around the developing lens capsule (tunica vasculosa lentis) (17). Hyaloid vessels naturally regress after birth, and regression is complete by postnatal day 30 (P30) (17). WT and PLCγ$^{+/-}$ mice were sacrificed at P1, P5, P10, P15, and P20; the eyes were enucleated; and the hyaloid vessels in approximately 10 serial sections were counted. It was not possible to perform these experiments on mice lacking both alleles of PLCγ because this genotype results in embryonic lethality (23). Despite only a 50% reduction of PLCγ, we observed a significant delay in the regression of the hyaloid vessels at days 1, 5 and 10 in the PLCγ$^{+/-}$ mice (Fig. 1A and B). While macrophages are essential for promoting regression of these vessels (21, 22), this did not seem to be the explanation for the delay in regression because at the P6 time point there were more macrophages associated with vessels in the PLCγ$^{+/-}$ mice than in controls (data not shown). Thus, developmentally programmed regression of the hyaloid vasculature was dependent on PLCγ.

To determine whether PLCγ contributed to regression of pathological vessels, we induced corneal neovascularization and focused on the regression of these neovessels. In wild-type mice, the bFGF-impregnated pellet (80 ng/pellet) induced peak neovascularization at day 7, and these vessels subsequently regressed within a 2-week time frame (Fig. 1C and D). The neovascular response was comparable in the PLCγ$^{+/-}$ mice, whereas regression was significantly delayed at both the 14- and 21-day time points (Fig. 1C and D). These results demonstrate that reducing the level of PLCγ expression in mice slowed developmental and pathological regression in at least certain vascular beds. We conclude that there was a good concordance between the *in vitro* model and two *in vivo* settings with respect to a role for PLCγ in regulating regression.

The mechanism by which PLCγ promotes regression involves more than just competing with PI3K for substrate. In our standard *in vitro* assay, endothelial cells organize into tubes (five to seven cells surrounding a lumen) (16), and this response is dependent on VEGF-A, which activates both phosphoinositide 3-kinase (PI3K) and PLCγ (14). While PI3K promoted formation of tubes, PLCγ destabilized tubes by

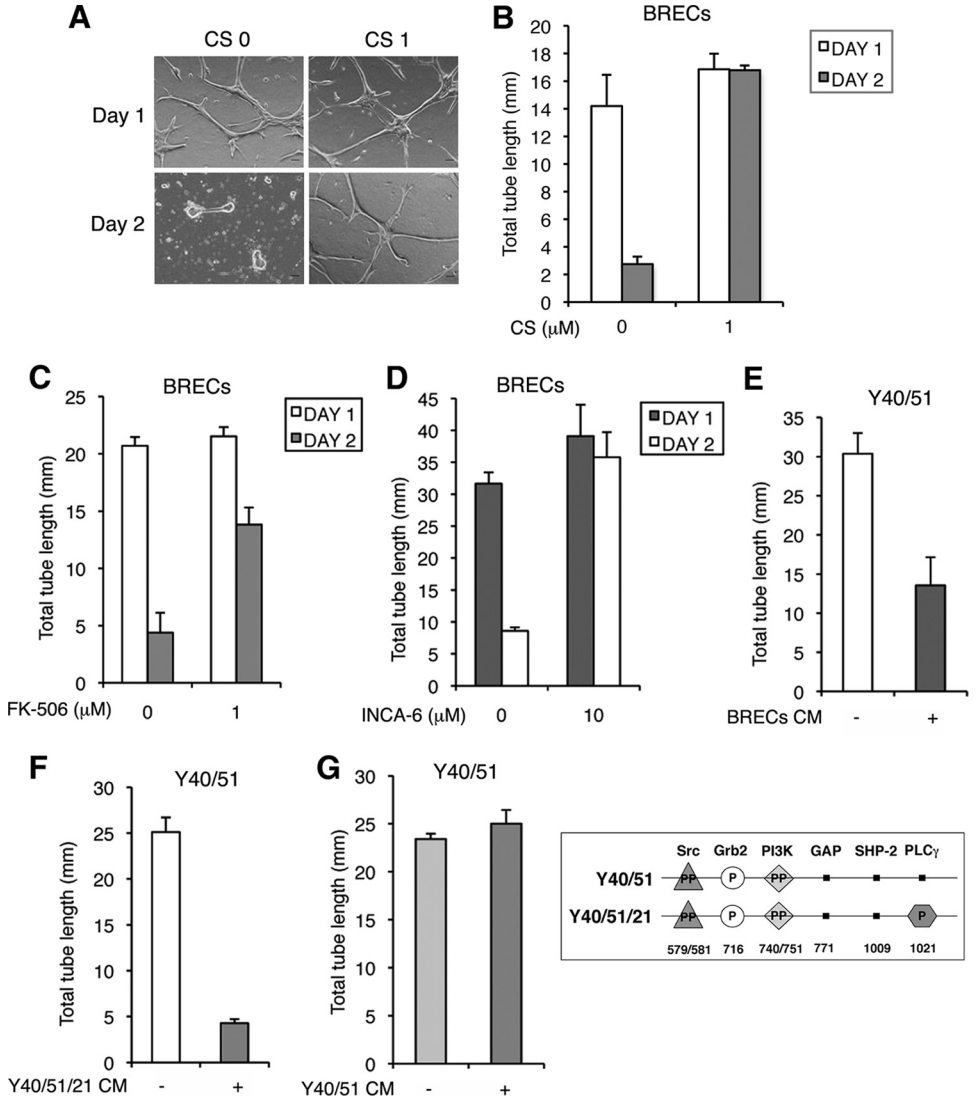

FIG. 2. Activation of the PLCγ/calcineurin pathway increases production of a secreted regression factor. BRECs were subjected to the standard VEGF-A-driven tube assay, and once tubes had formed, cyclosporine (CS) (1 μM) (A and B), FK-506 (1 μM) (C), INCA-6 (10 μM) (D), or buffer was added. After 24 h, three randomly selected fields were photographed (representative photos are shown in panel A) and tube lengths were measured (B to D). The bar graphs show the means ± standard deviations for three wells/treatment. (E to G) Conditioned medium experiments. To generate conditioned medium (CM), parental BRECs (E) or BRECs stably expressing either the Y40/51/21 PDGFR mutant (F) or the Y40/51 PDGFR mutant (G) were plated in a collagen sandwich gel, and then medium containing 2.5 ng/ml VEGF-A (only for parental BRECs) or buffer was added. Like most endothelial cells, BRECs express PDGF, and therefore introducing the PDGFR established an autocrine loop that drove spontaneous tube formation (14). After 48 h, CM was collected and added to 18- to 24-h-old cultures of tubes that had been independently generated using the Y40/51 cells. − indicates supplementation with mock conditioned medium that was generated in collagen sandwich gels that did not have cells. After 24 h, three randomly selected fields were photographed and tube lengths were measured. The bar graphs show the means ± standard deviations for three wells/treatment. (Bottom right) Diagram of the signaling proteins that bind to the PDGFR mutants used in this set of experiments (14); the Tyr phosphorylation sites that are required for binding are indicated. The filled squares symbolize tyrosine-to-phenylalanine mutations, whereas intact phosphorylation sites are represented by "P." The WT PDGFR associates with Src, Grb2, GAP, SHP-2, PI3K, and PLCγ. The Y40/51 mutant associates with Src, Grb2, and PI3K but not with GAP, SHP-2, or PLCγ. The Y40/51/21 mutant associates with Src, Grb2, PI3K, and PLCγ but not with GAP or SHP-2. The key difference between this pair of receptor mutants is that Y40/51/21 engages PLCγ, whereas Y40/51 does not.

competing with PI3K for their common substrate, phosphotidylinositide-4,5-bisphosphate (PtdIns-4,5-P_2) (14). Since PLCγ is also capable of initiating numerous signaling pathways, we considered whether these downstream events contributed to regression. While two general protein kinase C inhibitors (calphostin C and bisindolylmaleimide 1) had no effect on tube regression (data not shown), pharmacologically suppressing the activity of calcineurin (a calcium-regulated phosphatase downstream of PLCγ [12]) after tubes had formed greatly attenuated tube regression (Fig. 2A to D). In contrast to their effect on tube regression, the calcineurin inhibitors did not influence tube formation (Fig. 2A to D). These studies indicate that competition with PI3K was only a partial answer for how PLCγ facilitated tube regression and suggest that downstream signaling events were making an essential contribution.

If VEGF activates PLCγ, which promotes regression of

tubes, then why does VEGF also promote the formation of tubes (16)? One possibility was that PLCγ is not activated while tubes are forming; however, this appeared not to be the case (14). A second possibility is that PLCγ promotes the gradual production of a secreted regression factor; tubes could form while the level of the regression factor was low, but as the level increased, tubes regressed. We performed the following series of experiments to test whether the conditioned medium contained factors capable of inducing regression. We used not only the parental BRECs, in which tube formation was driven by endogenous VEGFRs that were activated by exogenously added VEGF-A, but also BRECs stably expressing the platelet-derived growth factor receptor (PDGFR) signaling mutants shown in Fig. 2 (bottom right). Like most endothelial cells, BRECs express PDGF, and introduction of PDGFR establishes an autocrine loop that promotes tube formation (VEGF is not required) (16). The reason to use this experimental system was that it enabled generation of stable tubes. Expression of a PDGFR mutant (Y40/51) that activated PI3K but not PLCγ resulted in stable tubes (14), which were used to test conditioned medium for regression activity. Medium from parental BRECs that had been cultured in the VEGF-A-driven tube assay for 48 h was collected and placed on stable tubes. As shown in Fig. 2E, this conditioned medium promoted regression of tubes, whereas conditioned medium collected from Y40/51 tubes did not (Fig. 2G). To test whether the presence of the regression activity in the conditioned medium was dependent on receptor-mediated activation of PLCγ, we compared conditioned medium from BRECs expressing PDGFRs that activate PI3K (Y40/51) with that from BRECs expressing PDGFRs that activate both PI3K and PLCγ (Y40/51/21). As shown in Fig. 2F and G, only the conditioned medium from the Y40/51/21 tubes induced regression. Taken together, these findings demonstrate that there was a regression factor in the conditioned medium and that its presence/activity was dependent on receptor-triggered activation of PLCγ.

Autotaxin induces regression of tubes. To identify the regression factor, we considered the events downstream of calcineurin. One of the calcineurin substrates is the transcription factor NFAT, which gains access to the nucleus following dephosphorylation by calcineurin (12). In the presence of INCA-6, which prevents calcineurin from interacting with NFAT, tubes failed to regress (Fig. 2D). These data suggested that the regression factor was an NFAT-regulated gene product. While there are many such genes, we considered autotaxin (ATX) for the following reasons. First, ATX is an NFAT-regulated gene (6). Second, ATX is essential for formation/remodeling of blood vessels during embryogenesis (41, 48). Similarly, purified ATX increases the vessel density of subcutaneously implanted Matrigel plugs (30). ATX's proangiogenic action could result from permitting vessels to form, enhancing their formation, preventing their regression, or a combination of these possibilities. Third, ATX is a motility factor for many cell types; inducing migration of cells within a tube would likely lead to its disorganization, which may be interpreted as regression in our tube assay.

We performed a series of experiments to test the idea that ATX was the regression factor, and the results strongly supported this concept. First, ATX gradually increased over the time course of the VEGF-A-driven tube assay (Fig. 3A); the same trend was observed for ATX mRNA (data not shown). Second, accumulation of ATX was dependent on activation of PLCγ; ATX accumulated in tubes that were organized from cells that could activate PLCγ but remained undetectable when the receptor could not activate PLCγ (Fig. 3A). Third, accumulation of ATX was inhibited when activation of calcineurin was blocked (Fig. 3A). Fourth, addition of an ATX inhibitor (L-histidine [10 mM]) (8) prevented regression of tubes, whereas control tubes (treated with L-glycine [10 mM]) regressed (Fig. 3B). Since highly specific ATX inhibitors are currently unavailable, we chose an siRNA-based approach to complement the inhibitor studies. When ATX expression was partially suppressed in HUVECs using siRNA, regression was attenuated (Fig. 3C). Fifth, recombinant, purified ATX (wild type [0.3 μg/ml]) induced regression of stable tubes (assembled from BRECs expressing the Y40/51 PDGFR), whereas the same dose of catalytically inactive ATX (T210A) induced regression poorly (Fig. 3D). Furthermore, HUVEC and BREC tubes organized in the presence of VEGF-A (which regress spontaneously) regressed faster in the presence of exogenously added catalytically active ATX than with the T210A mutant (data not shown). Taken together, the results of these experiments indicate that ATX was critically involved with regression of tubes.

Lysophosphatidic acid mediates tube regression. ATX is an enzyme that converts lysophosphatidylcholine (LPC) into lysophosphatidic acid (LPA); it can also hydrolyze sphingosylphosphorylcholine (SPC) to produce sphingosine-1-phosphate (S1P) (7). To test whether either of these ATX products were responsible for tube regression, we added each of them to the tube assay mixture after tubes had formed. LPA promoted regression of stable tubes (BRECs expressing Y40/51 PDGFR) in a concentration-dependent manner (Fig. 4A and data not shown). Furthermore, LPA accelerated spontaneous regression of tubes organized from parental BRECs and induced regression in CS-stabilized tubes (Fig. 4B and C). Time-lapse images show that LPA induced collapse of the tubes (Fig. 4D). In contrast, tube regression was insensitive to exogenously added S1P (Fig. 4E and F). These data indicate that LPA instead of S1P was the relevant ATX effector, and such a conclusion is consistent with the following four observations: (i) ATX hydrolyzes LPC more efficiently than SPC (7); (ii) the plasma level of LPC (the substrate for generating LPA) is >1,000 times higher than that of SPC (the substrate for generating S1P) (24); (iii) S1P is undetectable in embryos of mice missing both of the sphingosine kinase genes (29), which suggests that ATX does not contribute to S1P production *in vivo*; and (iv) the plasma concentration of S1P is unchanged in $ATX^{+/-}$ mice compared to $ATX^{+/+}$ mice, whereas that of LPA is reduced 50% (41, 48).

To pursue the idea that LPA was the critical ATX product, we overexpressed LPP1, a member of a family of lipid phosphate phosphatases (LPPs) that dephosphorylates LPA and thereby neutralizes it (26). BRECs that overexpressed LPP1 formed tubes normally in response to VEGF-A; however, they failed to regress (Fig. 4G). Moreover, purified ATX was unable to promote regression unless in the presence of purified LPC or serum (which is a source of LPC) (Fig. 4H and I and 3D). Finally, exogenously added LPA promoted migration of BRECs (Fig. 4J) and HUVECs (data not shown). Taken to-

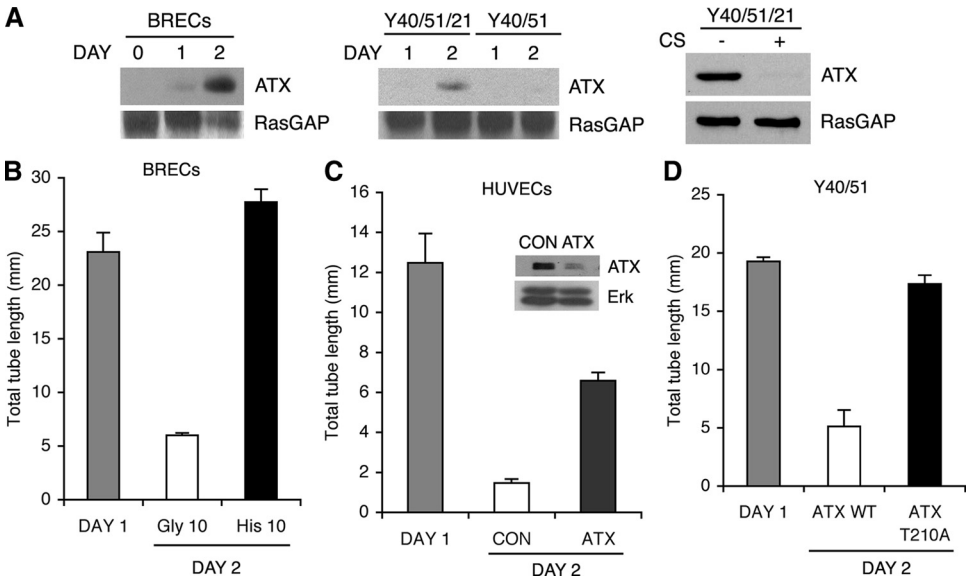

FIG. 3. ATX is necessary and sufficient for regression of tubes. (A) Parental BRECs or BRECs stably expressing the Y40/51/21 or Y40/51 PDGFR mutant were subjected to a tube assay with or without CS (1 μM). At the indicated times, total cell lysates were made and subjected to Western blot analysis using anti-ATX and anti-RasGAP antibodies; the Y40/51/21 cells shown in the right panel were harvested on day 2. Parallel experiments were performed on the conditioned medium, but we were unable to detect ATX. This may be due to factors such as the sensitivity of the ATX antibody, sequestration of ATX by the collagen gel, and/or degradation of secreted ATX in the context of a tube assay. (B) Parental BRECs were subjected to the standard VEGF-A-driven tube assay, and once the tubes had formed buffer, glycine (Gly) or L-histidine (His) was added to a final concentration of 10 mM. (C) HUVECs were transfected with either siRNA for ATX or nontargeting control siRNA (CON) and subjected to the VEGF-A-driven tube assay. The inset shows an anti-ATX Western blot of total cell lysates. The blot was reprobed with an anti-Erk antibody to verify equivalent protein loading. ATX expression was decreased by an average of 70% in siRNA ATX-transfected cells. (D) BRECs stably expressing the Y40/51 PDGFR mutant were subjected to a tube assay. Once tubes were formed, purified wild-type ATX (0.3 μg/ml) or inactive mutant ATX T210A (0.3 μg/ml) was added. After 24 h, three randomly selected fields were photographed and tube lengths were measured. The bar graphs show the means ± standard deviations for three wells/treatment.

gether, these data indicate that LPA was the critical ATX product.

Regression is accelerated in ATX transgenic mice. Since ATX regulated tube regression in our *in vitro* model system, we considered whether ATX contributed to regression of blood vessels *in vivo*. To this end, we compared hyaloid vessel regression in wild-type and ATX transgenic mice. The transgene is driven by the α1-antitrypsin promoter, and the plasma level of ATX was elevated (1.3- to 3.6-fold). Similarly, the transgenic mice had increased amounts of ATX activity and LPA in their plasma (32). These mice are fertile and have no overt phenotype with the exceptions of bleeding diathesis and attenuation of thrombosis. The overall development of the eye was comparable in the wild-type and transgenic mice (Fig. 5A). In contrast, regression of hyaloid vessels was accelerated in transgenic mice at days 1 and 3 (Fig. 5B). These observations indicate that an increase in the circulating level of ATX/LPA promoted regression of blood vessels *in vivo*.

DISCUSSION

We previously observed that PLCγ was required for regression of tubes in an *in vitro* assay (14). In this study we extended this observation to the *in vivo* setting: regression of developmental and pathological blood vessels was delayed in mice heterozygous for PLCγ. In the *in vitro* setting, ATX/LPA appeared to be the effectors of PLCγ-directed regression, and in the *in vivo* setting, increasing the circulating level of ATX/LPA promoted regression of hyaloid vessels.

The fact that there are two sources of ATX/LPA, intrinsic and extrinsic, leads to the question of which of them is responsible for driving regression. Our data in the *in vitro* setting suggest that both are important. Knocking down the cell's ability to make ATX blunted regression (Fig. 3C), even though this manipulation presumably did not alter that amount of ATX present in the serum-containing medium. Thus, cell-produced ATX was contributing. On the other hand, tubes regressed in response to exogenously added LPA. Furthermore, in the absence of serum-containing medium, tubes did not regress, even though they made ATX, and adding LPC (so that they could generate LPA) did not promote regression (unpublished observation). This combination may have resulted in insufficient LPA production, since increasing the amount of ATX (by adding purified ATX) induced regression. We concluded that both extrinsic and intrinsic sources of ATX/LPA were contributing to regression of tubes, and the combined input may be necessary to bring the level of LPA above the threshold required to drive regression.

In the *in vivo* setting, we observed that increasing the circulating level of ATX was sufficient to accelerate regression of hyaloid vessels (Fig. 5). However, this appears not to be the only way to regulate regression of this vascular bed. There was no difference in the plasma level of ATX in PLCγ$^{+/+}$ and PLCγ$^{+/-}$ pups at the P6 time point (unpublished observations)

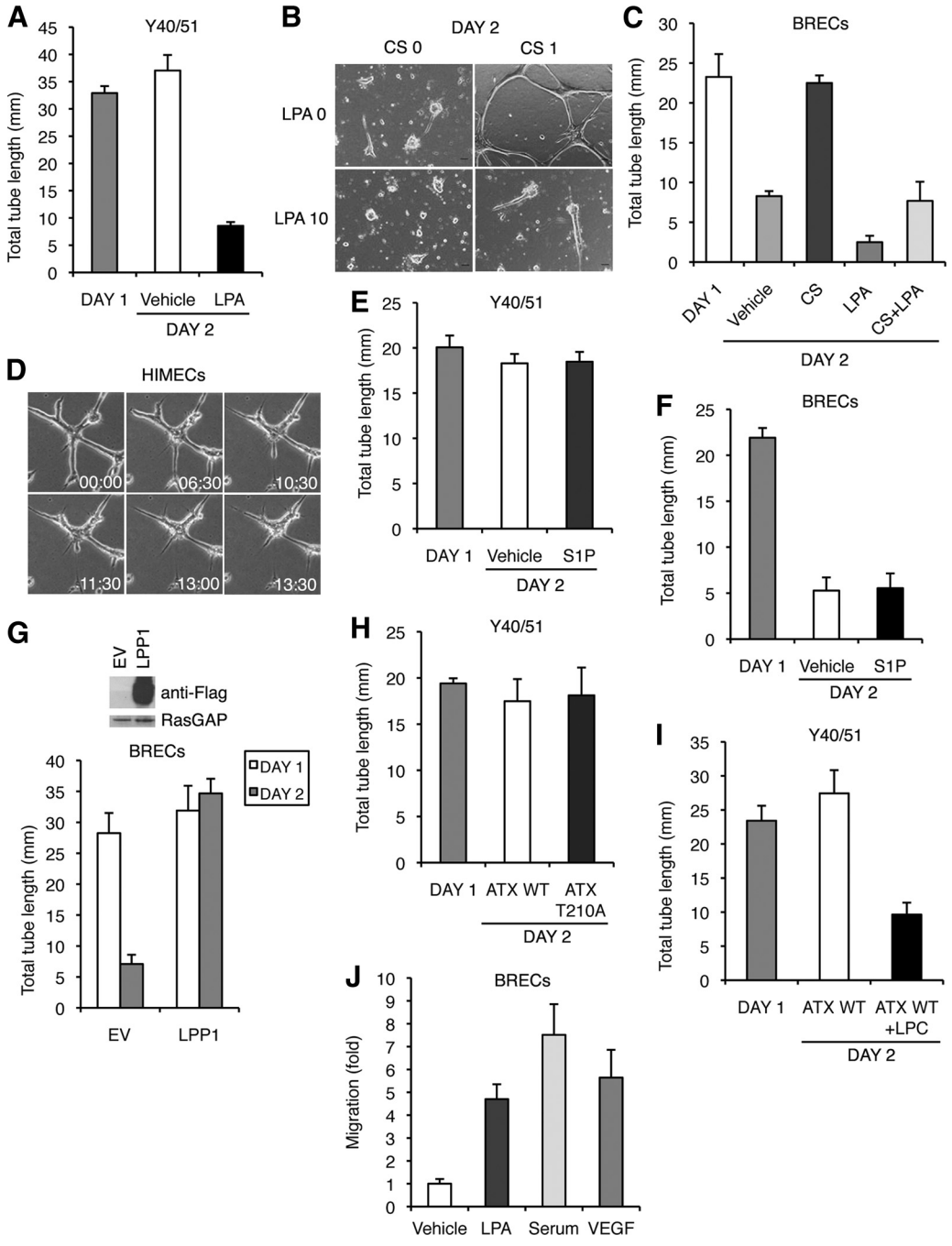

FIG. 4. The ATX product LPA is responsible for tube regression. (A) BRECs stably expressing the Y40/51 PDGFR mutant were subjected to a tube assay. After 24 h, fresh medium containing 10 μM LPA or buffer was added. (B and C) Parental BRECs were subjected to the standard VEGF-A-driven tube assay. Once the tubes had formed, buffer, LPA (10 μM), and/or cyclosporine (1 μM) was added. (D) HIMECs were subjected to a tube assay. After 6 h, LPA (10 μM) was added to the culture medium. Time-lapse images of tubes were captured, and serial images are presented. (E) Same as panel A, expect that S1P (10 μM) was added instead of LPA. (F) Same as panel E, expect that parental BRECs were using instead of the BRECs expressing the Y40/51 PDGFR mutant. (G) BRECs stably expressing LPP1 were subjected to the standard VEGF-A-driven tube assay. The inset is an anti-Flag Western blot of lysates prepared from empty vector (EV) or LPP1-expressing cells; the RasGAP blot is induced as a loading control. (H) BRECs stably expressing the Y40/51 PDGFR mutant were subjected to a tube assay. This experiment differed from the standard tube assay in that serum-free medium was used instead of medium containing 10% horse serum. Purified WT ATX (0.3 μg/ml) or inactive mutant ATX T210A (0.3 μg/ml) was added once the tubes had formed (at the 18- to 24-h time point), and the tube lengths were measured after 18 to 24 h of exposure to ATX. (I) Same as panel H, expect that ATX and LPC (10 μM) were added instead of catalytically inactive ATX. (J) BRECs were subjected to a migration assay using a Boyden chamber in the presence or absence of 1 μM LPA. The migrating cells were quantified as described in Materials and Methods. The means ± standard deviations from three independent experiments are presented in the bar graph.

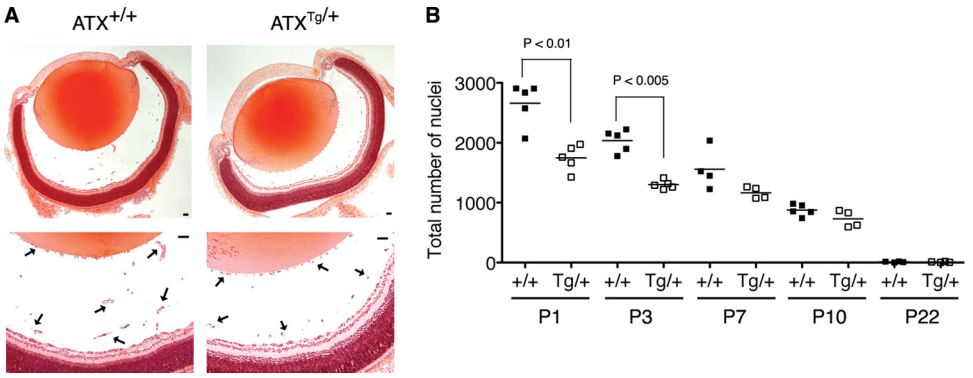

FIG. 5. Regression of hyaloid vessels is accelerated in $ATX^{Tg/+}$ mice. (A) At postnatal days 1, 3, 7, 10, and 22, mice were euthanized, and the eyes were removed, fixed, and sectioned. Sections were stained with hematoxylin and eosin, and representative sections prepared from P1 mice are shown; the lower panels are high-magnification photos in which arrows point to the hyaloid vessels. The bar is 50 μm. (B) The nuclei within hyaloid vessels were counted as described in Materials and Methods, and the result for each eye is shown. There was a statistically significant difference between the two groups at the first two time points.

even though regression was faster in the $PLC\gamma^{+/+}$ mice. We were unable to measure the amount of ATX protein in hyaloid vessels (unpublished observations), and it remains an open question whether the amount of ATX produced by these cells is associated with the difference in the rate of regression between the two genotypes. Responsiveness to LPA is also dependent on additional variables such as the presence of LPA inhibitors, the expression and activity of LPPs, and the type and level of LPA receptors expressed (39, 47). Further studies are required to determine the underlying reason for delayed regression of hyaloid vessels in the $PLC\gamma^{+/-}$ mice.

The most common mechanism thought to account for vessel regression is growth factor deprivation-induced apoptosis. Pathological vessels in tumors and within numerous ocular beds undergo at least partial regression in response to anti-VEGF therapy (5). Regression can also be induced by the microenvironment of the vasculature, and this information can come in the form of soluble factors that are produced by other cell types (13). Thus, there appear to be multiple ways to induce regression of vessels; this information is likely to guide efforts to enhance current antiangiogenic therapies.

Our findings indicate that endothelial cells within a tube can generate factors that promote their destabilization, which in certain settings can lead to regression. We call this pathway the intrinsic destabilization pathway (IDP) (Fig. 6). The key events in this pathway include activation of PLCγ, which leads to increased production of ATX/LPA. LPA acts through its cell surface receptors to activate RhoA/ROCK and induce a variety of cellular responses, including motility, which should destabilize the cell-cell interactions needed to maintain organization within tubes/vessels and thereby facilitate regression. Time-lapse studies indicate that as tubes regressed, they first collapsed (Fig. 4D) and then underwent apoptosis (14).

Since proangiogenic factors such as VEGF and bFGF activated PLCγ (and hence the IDP), why are these agents best known for their ability to facilitate the formation of new vessels instead of inducing their regression? We speculate that activation of the IDP results in destabilization of a stable vascular bed and hence is an essential, early step in the formation of new vessels. Activation of the IDP in an unstable vascular bed (newly formed or compromised due to diabetes-induced loss of pericytes that occurs in the retina) would result in regression. Thus, the state of the vascular bed may determine whether engaging the IDP promotes angiogenesis versus regression.

How does the IDP relate to our earlier findings that PLCγ induces regression by competing with PI3K for substrate? We previously focused on PLCγ's ability to reduce the output of PI3K/Akt as a means to attenuate signaling events necessary for tube formation and stability (14). An additional consequence of the increased consumption of PtdIns-4,5-P_2 by PLCγ would be production of regression factors such as ATX/LPA. The discovery of the IDP reveals that PLCγ not only reduces the output of PI3K (and thereby limits tube formation) but also initiates a series of events that leads to production of secreted regression factors.

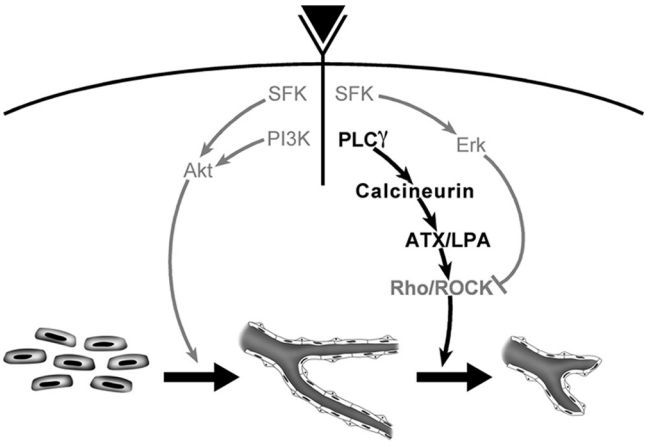

FIG. 6. Schematic diagram of the intrinsic destabilization pathway (IDP). Angiogenic growth factor receptors engage PLCγ, which activates calcineurin and leads to an increase in ATX. ATX is a secreted form of phospholipase D, which converts lysophosphatidylcholine into lysophosphatidic acid (LPA). We postulate that an increase in LPA drives regression by first promoting migration of endothelial cells, which destabilizes/disorganizes the vessel. The events shown in bold are the focus of this report, while those in gray are from previous publications (14, 15), and control tube formation or regression.

Our findings that hyaloid vessel regression was aberrant in mice that under- or overexpress members of the IDP lead to the question of how this relates to Wnt- and Ang2-dependent events, which regulate regression of this vascular bed (35). In other settings, Wnts regulate the level of ATX (18, 34) and induce ATX in tumors (19, 42, 49). Whether Wnts and/or Ang2 control the level and/or activity of ATX in vascular endothelial cells is an open question. Alternatively, Wnts and Ang2 may influence the expression of LPA receptors or the ability of these receptors to induce the signaling events that are required for regression (such as Rho/ROCK activation [15, 28]). Furthermore, while our findings support a role for ATX/LPA, they do not rule out the involvement of other regression factors. Ongoing studies are focused on addressing these questions.

ACKNOWLEDGMENTS

We are very grateful to Susan Pyne (Strathcylde Institute of Pharmacy and Biomedical Science, Glasgow, United Kingdom) for the LPP1 construct and to Demin Wang and James Schuman for providing the PLC$\gamma^{+/+}$ and PLC$\gamma^{+/-}$ mice.

This study was supported by a Young Clinical Scientist Award from the Flight Attendant Medical Research Institute (to E.I.), NIH/NIDDK grant 1KO1 DK083336 (to E.I.), NIH grant EY016385 (to A.K.), and Pew Latin American Fellows Program in the Biomedical Sciences and American Diabetes Association Mentor-Based Minority Postdoctoral Fellowship 7-09-MI-04 (to J.A.). This research was also supported in part by the Intramural Research Program of the National Institutes of Health, National Cancer Institute, and Center for Cancer Research (to T.C. and M.S.).

REFERENCES

1. **Ausprunk, D. H., K. Falterman, and J. Folkman.** 1978. The sequence of events in the regression of corneal capillaries. Lab. Invest. **38:**284–294.
2. **Avery, R. L., D. J. Pieramici, M. D. Rabena, A. A. Castellarin, M. A. Nasir, and M. J. Giust.** 2006. Intravitreal bevacizumab (Avastin) for neovascular age-related macular degeneration. Ophthalmology **113:**363–372.
3. **Benjamin, L. E., D. Golijanin, A. Itin, D. Pode, and E. Keshet.** 1999. Selective ablation of immature blood vessels in established human tumors follows vascular endothelial growth factor withdrawal. J. Clin. Invest. **103:**159–165.
4. **Binion, D. G., G. A. West, K. Ina, N. P. Ziats, S. N. Emancipator, and C. Fiocchi.** 1997. Enhanced leukocyte binding by intestinal microvascular endothelial cells in inflammatory bowel disease. Gastroenterology **112:**1895–1907.
5. **Carmeliet, P.** 2005. Angiogenesis in life, disease and medicine. Nature **438:**932–936.
6. **Chen, M., and K. L. O'Connor.** 2005. Integrin alpha6beta4 promotes expression of autotaxin/ENPP2 autocrine motility factor in breast carcinoma cells. Oncogene **24:**5125–5130.
7. **Clair, T., J. Aoki, E. Koh, R. W. Bandle, S. W. Nam, M. M. Ptaszynska, G. B. Mills, E. Schiffmann, L. A. Liotta, and M. L. Stracke.** 2003. Autotaxin hydrolyzes sphingosylphosphorylcholine to produce the regulator of migration, sphingosine-1-phosphate. Cancer Res. **63:**5446–5453.
8. **Clair, T., E. Koh, M. Ptaszynska, R. W. Bandle, L. A. Liotta, E. Schiffmann, and M. L. Stracke.** 2005. L-Histidine inhibits production of lysophosphatidic acid by the tumor-associated cytokine, autotaxin. Lipids Health Dis. **4:**5–17.
9. **Eter, N., T. U. Krohne, and F. G. Holz.** 2006. New pharmacologic approaches to therapy for age-related macular degeneration. BioDrugs **20:**167–179.
10. **Gitlin, J. D., and P. A. D'Amore.** 1983. Culture of retinal capillary cells using selective growth media. Microvasc. Res. **26:**74–80.
11. **Gragoudas, E. S., A. P. Adamis, E. T. J. Cunningham, M. Feinsod, D. R. Guyer, and the VEGF Inhibition Study in Ocular Neovascularization Clinical Trial Group.** 2004. Pegaptanib for neovascular age-related macular degeneration. N. Engl. J. Med. **351:**2805–2816.
12. **Hogan, P. G., L. Chen, J. Nardone, and A. Rao.** 2003. Transcriptional regulation by calcium, calcineurin, and NFAT. Genes Dev. **17:**2205–2232.
13. **Im, E., and A. Kazlauskas.** 2006. New insights regarding vessel regression. Cell Cycle **5:**2057–2059.
14. **Im, E., and A. Kazlauskas.** 2006. Regulating angiogenesis at the level of PtdIns-4,5-P2. EMBO J. **25:**2075–2082.
15. **Im, E., and A. Kazlauskas.** 2007. Src family kinases promote vessel stability by antagonizing the Rho/ROCK pathway. J. Biol. Chem. **282:**29122–29129.
16. **Im, E., A. Venkatakrishnan, and A. Kazlauskas.** 2005. Cathepsin B regulates the intrinsic angiogenic threshold of endothelial cells. Mol. Biol. Cell **16:**3488–3500.
17. **Ito, M., and M. Yoshioka.** 1999. Regression of the hyaloid vessels and pupillary membrane of the mouse. Anat. Embryol. (Berl.) **200:**403–411.
18. **Kehlen, A., R. Lauterbach, A. N. Santos, K. Thiele, U. Kabisch, E. Weber, D. Riemann, and J. Langner.** 2001. IL-1 beta- and IL-4-induced down-regulation of autotaxin mRNA and PC-1 in fibroblast-like synoviocytes of patients with rheumatoid arthritis (RA). Clin. Exp. Immunol. **123:**147–154.
19. **Kenny, P. A., T. Enver, and A. Ashworth.** 2005. Receptor and secreted targets of Wnt-1/beta-catenin signalling in mouse mammary epithelial cells. BMC Cancer **5:**3.
20. **Kenyon, B. M., E. E. Voest, C. C. Chen, E. Flynn, J. Folkman, and R. J. D'Amato.** 1996. A model of angiogenesis in the mouse cornea. Invest. Ophthalmol. Vis. Sci. **37:**1625–1632.
21. **Lang, R., M. Lustig, F. Francois, M. Sellinger, and H. Plesken.** 1994. Apoptosis during macrophage-dependent ocular tissue remodelling. Development **120:**3395–3403.
22. **Lang, R. A., and J. M. Bishop.** 1993. Macrophages are required for cell death and tissue remodeling in the developing mouse eye. Cell **74:**453–462.
23. **Liao, H. J., T. Kume, C. McKay, M. J. Xu, J. N. Ihle, and G. Carpenter.** 2002. Absence of erythrogenesis and vasculogenesis in Plcg1-deficient mice. J. Biol. Chem. **277:**9335–9341.
24. **Liliom, K., G. Sun, M. Bunemann, T. Virag, N. Nusser, D. L. Baker, D. A. Wang, M. J. Fabian, B. Brandts, K. Bender, A. Eickel, K. U. Malik, D. D. Miller, D. M. Desiderio, G. Tigyi, and L. Pott.** 2001. Sphingosylphosphocholine is a naturally occurring lipid mediator in blood plasma: a possible role in regulating cardiac function via sphingolipid receptors. Biochem. J. **355:**189–197.
25. **Lobov, I. B., S. Rao, T. J. Carroll, J. E. Vallance, M. Ito, J. K. Ondr, S. Kurup, D. A. Glass, M. S. Patel, W. Shu, E. E. Morrisey, A. P. McMahon, G. Karsenty, and R. A. Lang.** 2005. WNT7b mediates macrophage-induced programmed cell death in patterning of the vasculature. Nature **437:**417–421.
26. **Long, J. S., K. Yokoyama, G. Tigyi, N. J. Pyne, and S. Pyne.** 2006. Lipid phosphate phosphatase-1 regulates lysophosphatidic acid- and platelet-derived-growth-factor-induced cell migration. Biochem. J. **394:**495–500.
27. **Matsumoto, T., and L. Claesson-Welsh.** 2001. VEGF receptor signal transduction. Sci. STKE **2001:**RE21.
28. **Mavria, G., Y. Vercoulen, M. Yeo, H. Paterson, M. Karasarides, R. Marais, D. Bird, and C. J. Marshall.** 2006. ERK-MAPK signaling opposes Rho-kinase to promote endothelial cell survival and sprouting during angiogenesis. Cancer Cell **9:**33–44.
29. **Mizugishi, K., T. Yamashita, A. Olivera, G. F. Miller, S. Spiegel, and R. L. Proia.** 2005. Essential role for sphingosine kinases in neural and vascular development. Mol. Cell. Biol. **25:**11113–11121.
30. **Nam, S. W., T. Clair, Y. S. Kim, A. McMarlin, E. Schiffmann, L. A. Liotta, and M. L. Stracke.** 2001. Autotaxin (NPP-2), a metastasis-enhancing motogen, is an angiogenic factor. Cancer Res. **61:**6938–6944.
31. **Ory, D. S., B. A. Neugeboren, and R. C. Mulligan.** 1996. A stable human-derived packaging cell line for production of high titer retrovirus/vesicular stomatitis virus G pseudotypes. Proc. Natl. Acad. Sci. U. S. A. **93:**11400–11406.
32. **Pamuklar, Z., L. Federico, S. Liu, M. Umezu-Goto, A. Dong, M. Panchatcharam, Z. Fulerson, E. Berdyshev, V. Natarajan, X. Fang, L. A. van Meeteren, W. H. Moolenaar, G. B. Mills, A. J. Morris, and S. S. Smyth.** 2009. Autotaxin/lysopholipase D and lysophosphatidic acid regulate murine hemostasis and thrombosis. J. Biol. Chem. **284:**7385–7394.
33. **Phng, L. K., M. Potente, J. D. Leslie, J. Babbage, D. Nyqvist, I. Lobov, J. K. Ondr, S. Rao, R. A. Lang, G. Thurston, and H. Gerhardt.** 2009. Nrarp coordinates endothelial Notch and Wnt signaling to control vessel density in angiogenesis. Dev. Cell **16:**70–82.
34. **Ptaszynska, M. M., M. L. Pendrak, R. W. Bandle, M. L. Stracke, and D. D. Roberts.** 2008. Positive feedback between vascular endothelial growth factor-A and autotaxin in ovarian cancer cells. Mol. Cancer Res. **6:**352–363.
35. **Rao, S., I. B. Lobov, J. E. Vallance, K. Tsujikawa, I. Shiojima, S. Akunuru, K. Walsh, L. E. Benjamin, and R. A. Lang.** 2007. Obligatory participation of macrophages in an angiopoietin 2-mediated cell death switch. Development **134:**4449–4458.
36. **Rogers, M. S., R. M. Rohan, A. E. Birsner, and R. J. D'Amato.** 2004. Genetic loci that control the angiogenic response to basic fibroblast growth factor. FASEB J. **18:**1050–1059.
37. **Sakurai, Y., K. Ohgimoto, Y. Kataoka, N. Yoshida, and M. Shibuya.** 2005. Essential role of Flk-1 (VEGF receptor 2) tyrosine residue 1173 in vasculogenesis in mice. Proc. Natl. Acad. Sci. U. S. A. **102:**1076–1081.
38. **Saunders, W. B., B. L. Bohnsack, J. B. Faske, N. J. Anthis, K. J. Bayless, K. K. Hirschi, and G. E. Davis.** 2006. Coregulation of vascular tube stabilization by endothelial cell TIMP-2 and pericyte TIMP-3. J. Cell Biol. **175:**179–191.
39. **Sciorra, V. A., and A. J. Morris.** 2002. Roles for lipid phosphate phosphatases in regulation of cellular signaling. Biochim. Biophys. Acta **1582:**45–51.
40. **Takahashi, T., S. Yamaguchi, K. Chida, and M. Shibuya.** 2001. A single autophosphorylation site on KDR/Flk-1 is essential for VEGF-A-dependent

activation of PLC-gamma and DNA synthesis in vascular endothelial cells. EMBO J. **20:**2768–2778.

41. **Tanaka, M., S. Okudaira, Y. Kishi, R. Ohkawa, S. Iseki, M. Ota, S. Noji, Y. Yatomi, J. Aoki, and H. Arai.** 2006. Autotaxin stabilizes blood vessels and is required for embryonic vasculature by producing lysophosphatidic acid. J. Biol. Chem. **281:**25822–25830.
42. **Tice, D. A., W. Szeto, I. Soloviev, B. Rubinfeld, S. E. Fong, D. L. Dugger, J. Winer, P. M. Williams, D. Wieand, V. Smith, R. H. Schwall, D. Pennica, and P. Polakis.** 2002. Synergistic induction of tumor antigens by Wnt-1 signaling and retinoic acid revealed by gene expression profiling. J. Biol. Chem. **277:** 14329–14335.
43. **Tokumura, A., E. Majima, Y. Kariya, K. Tominaga, K. Kogure, K. Yasuda, and K. Fukuzawa.** 2002. Identification of human plasma lysophospholipase D, a lysophosphatidic acid-producing enzyme, as autotaxin, a multifunctional phosphodiesterase. J. Biol. Chem. **277:**39436–39442.
44. **Umezu-Goto, M., Y. Kishi, A. Taira, K. Hama, N. Dohmae, K. Takio, T. Yamori, G. B. Mills, K. Inoue, J. Aoki, and H. Arai.** 2002. Autotaxin has lysophospholipase D activity leading to tumor cell growth and motility by lysophosphatidic acid production. J. Cell Biol. **158:**227–233.
45. **Valius, M., C. Bazenet, and A. Kazlauskas.** 1993. Tyrosines 1021 and 1009 are phosphorylation sites in the carboxy terminus of the platelet-derived growth factor receptor beta subunit and are required for binding of phospholipase C gamma and a 64-kilodalton protein, respectively. Mol. Cell. Biol. **13:**133–143.
46. **Valius, M., and A. Kazlauskas.** 1993. Phospholipase C-gamma 1 and phosphatidylinositol 3 kinase are the downstream mediators of the PDGF receptor's mitogenic signal. Cell **73:**321–334.
47. **van Meeteren, L. A., and W. H. Moolenaar.** 2007. Regulation and biological activities of the autotaxin-LPA axis. Prog. Lipid Res. **46:**145–160.
48. **van Meeteren, L. A., P. Ruurs, C. Stortelers, P. Bouwman, M. A. van Rooijen, J. P. Pradère, T. R. Pettit, M. J. Wakelam, J. S. Saulnier-Blache, C. L. Mummery, W. H. Moolenaar, and J. Jonkers.** 2006. Autotaxin, a secreted lysophospholipase D, is essential for blood vessel formation during development. Mol. Cell. Biol. **26:**5015–5022.
49. **Zirn, B., B. Samans, S. Wittmann, T. Pietsch, I. Leuschner, N. Graf, and M. Gessler.** 2006. Target genes of the WNT/beta-catenin pathway in Wilms tumors. Genes Chromosomes Cancer **45:**565–574.